Screening of Heterogeneous Multimetallic Nanoparticle Catalysts Supported on Metal Oxides for Mono-, Poly-, and Heteroaromatic Hydrogenation Activity
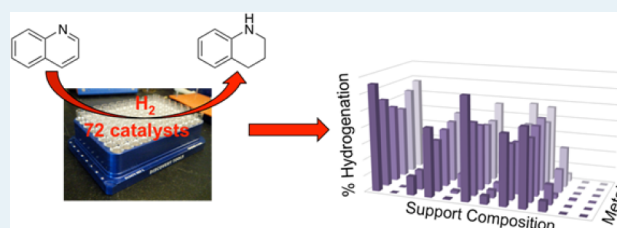
Nicole A. Beckers, Steven Huynh, Xiaojiang Zhang, Erik J. Luber, and Jillian M. Buriak*

Department of Chemistry, University of Alberta and the National Institute for Nanotechnology (NRC-NINT), Edmonton, Alberta, Canada T6G 2G2

⬢ *Supporting Information*

ABSTRACT: A series of oxide supported mono-, bi-, and trimetallic nanoparticle catalysts were synthesized and screened for catalytic activity for the hydrogenation of mono-, poly-, and heteroaromatic substrates. Seventy-two different catalysts were screened for catalytic activity for the hydrogenation of toluene, naphthalene, pyridine, indole, quinoline, thiophene, and benzothiophene under mild conditions; five of these seven substrates were successfully hydrogenated under the reaction conditions. Bulk kinetic studies, including temperature and pressure studies, were performed using select catalysts for the hydrogenation of one hydrocarbon (naphthalene) and one-heteroatom substituted-substrate (quinoline). A quinoline loading study was also conducted in which the ratio of substrate/ catalyst was varied. Standard materials characterization techniques including transmission electron microscopy (TEM), X-ray photoelectron spectroscopy (XPS), and X-ray diffraction (XRD) were also used to acquire information about the size, oxidation state, and crystallinity of the nanoparticle catalysts.

KEYWORDS: nanoparticles, catalysis, hydrogenation, quinoline, combinatorial, naphthalene

INTRODUCTION

Arene hydrogenation is a challenging catalytic reaction under ambient conditions because of the stability of the aromatic rings. Bitumen, the hydrocarbon product of the enormous oil sand deposits in Alberta and around the world, is a compendium of large polyaromatic hydrocarbon molecules.[1-3] To upgrade and transform bitumen into synthetic crude oil, it must be hydrogenated and further converted, a series of reactions of great importance to the petrochemical industry.[4-7] Harsh conditions are typically required for the hydrogenation of polyaromatic hydrocarbons to obtain complete (deep) hydrogenation of all the aromatic rings.[7] These rather extreme conditions, however, lead to inevitable catalyst deactivation, particularly in the presence of impurities and poisons.[7-9] Hydrogenation of polyaromatic and heteroaromatic molecules present another set of challenges, in addition to the difficulties related to breaking aromaticity. In the case of heteroaromatic hydrogenation, there is potential for the heteroatom-containing substrate itself, particularly if it contains nitrogen or sulfur, to behave as a poison toward the metal catalyst, leading to catalyst deactivation. Catalyst replacement and disposal is costly, and thus there is strong interest in the discovery and development of new families of active catalysts that can withstand the presence of heteroatoms, and function under less extreme conditions.

Aromatic hydrogenation has been previously studied using a variety of prepared solution phase and supported nanoparticle catalysts.[7,9-83] Nanoparticle (NP) catalysts have shown to be advantageous for a variety of reasons, including high surface areas and energies, unique electronic effects, and potentially lower cost.[84,85] For aromatic hydrogenation, the most widely studied substrates are benzene and toluene, and a number of different late transition metal NP-based catalyst systems that function under ambient conditions (1 atm, 298 K) have been prepared and characterized.[21,22,30-32,73,80,86] In terms of polyaromatics under ambient conditions, however, there have been far fewer studies. For example, Park and co-workers used Rh NPs on aluminum oxyhydroxide nanofibers for the hydrogenation of naphthalene to tetralin and anthracene to 9,10-dihydroanthracene at room temperature with a hydrogen balloon (~1 atm pressure),[17] and tetrahedral and spherical Rh NPs on charcoal have been used for the hydrogenation of naphthalene and anthracene under ambient conditions.[73] Naphthalene has also been hydrogenated at 1 atm hydrogen pressure to tetralin with a Pd/C catalyst in the presence of an ionic liquid additive,[32] but it has been a challenge to further hydrogenate this compound to decahydronaphthalene (deca-lin) under these gentle conditions.[17,66] In another approach, a compound catalyst consisting of mononuclear rhodium complexes tethered to a heterogeneous Pd-SiO$_2$ catalyst was

active under ambient conditions (40 °C, 1 atm H_2) for the hydrogenation of naphthalene to both tetralin (88% yield) and decalin (12% yield).[66] The ambient hydrogenation (25 °C, < 10 atm H_2) of anthracene has also been investigated using a number of NP-based systems, including Rh NPs on aluminum oxyhydroxide nanofibers as mentioned earlier,[17] tetrahedral and spherical Rh NPs on charcoal,[73] and others.[16,32,77,87]

With respect to nitrogen- and sulfur-containing heteroaromatic compounds, there are limited examples in the literature regarding mild hydrogenation conditions using metal NP catalysts. To hydrogenate quinoline, Sánchez-Delgado and co-workers used poly(4-vinylpyridine)-immobilized Ru NPs at 120 or 150 °C and pressures of 10−50 atm H_2.[88,89] Grobas et al. used Pd/C in formic acid at 28 °C and atmospheric pressure,[90] and Park et al. used Rh NPs on aluminum oxyhydroxide nanofibers at room temperature and 1 atm pressure,[17] yielding almost exclusively 1,2,3,4-tetrahydroquinoline as the sole product in all cases. Mévellec and co-workers also used Rh NPs to hydrogenate a variety of substrates including pyridine to piperidine and quinoline to 1,2,3,4-tetrahydroquinoline at 1 atm H_2 and 20 °C.[91] Mao et al. used Pd NPs on tannin grafted collagen fibers to hydrogenate quinoline to 1,2,3,4-tetrahydroquinoline between 20 and 80 °C and 10−40 atm H_2.[92]

Mixed metal systems such as bimetallic catalysts have been shown to have, under certain conditions, enhanced activity and selectivity, and an increased tolerance to nitrogen and sulfur containing compounds when compared to their monometallic counterparts.[93−96] For example, Yoon et al. demonstrated that a bimetallic RhPd/CNT catalyst had an unusually high catalytic activity for the hydrogenation of anthracene at 10 atm H_2 and 25 °C when compared to the monometallic Rh/CNT and Pd/CNT catalysts.[16] Venezia et al. showed that a Au−Pd/SiO₂−Al₂O₃ catalyst had a high turnover frequency for the hydrogenation of toluene in the presence of dibenzothiophene.[55] In 2009, Yoon et al. also showed while Rh/CNT and Pd/CNT catalysts had low activities for the room temperature hydrogenation of benzene, the Pd−Rh/CNT catalyst was much more active.[15] These tantalizing results support the concept that mixed metal NP systems may have substantially different catalytic characteristics when compared with their monometallic parent NP catalysts.

Because the number of combinations of bimetallic and polymetallic systems is far larger than could be reasonably screened for catalytic activity via empirical methods, combinatorial methods may be useful in providing leads to active mixtures. The combinatorial screening of catalytically active materials has become a very broad area of research, ranging from heterogeneous water splitting catalysts, to automobile emissions control, to catalysts for bulk and fine chemical production, among others.[97−112] For the hydrogenation of organic compounds, libraries of supported mixed metal materials have been prepared and screened against a number of hydrocarbon substrates, including 1-hexyne and toluene.[98] Thus, the potential for combinatorial screening of hydrogenation catalysts for the discovery of new leads and catalyst optimization is large.

In this work, a series of mono-, bi-, and trimetallic NP catalysts supported on metal oxides were synthesized and screened for the hydrogenation of several polyaromatic and heteroaromatic substrates; in this way, several variables were simultaneously investigated, including metal NP and oxide support composition. To build upon the concepts stated earlier with regards to heterogeneous mixed-metal NP systems, the goal of this work was the elucidation of catalysts active for the hydrogenation of N- or S-containing heteroaromatic substrates under mild conditions, with higher activities and sulfur and nitrogen tolerance than their monometallic counterparts. The aromatic substrates and their possible hydrogenation products are outlined in Scheme 1. To attempt to identify new leads for

Scheme 1. Aromatic Substrates and the Observed Hydrogenation Products As Determined by GC-MS Analysis
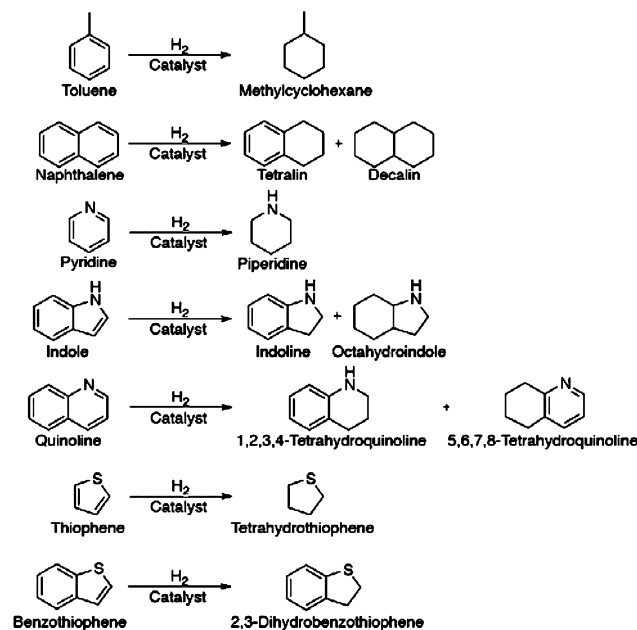
supported mixed-metal heterogeneous NP-based catalysis, we prepared 72 different catalysts (6 NP compositions × 12 metal oxide supports), and screened them against 7 organic aromatic substrates, resulting in 504 distinct reactions.

■ EXPERIMENTAL SECTION

Materials. RuCl₃·xH₂O (99.9%-Ru), IrCl₃·xH₂O (99.9%-Ir), Na₂PtCl₄·xH₂O, RhCl₃·xH₂O (38−41% Rh), and 0.5% Rh/Al₂O₃ (pellets) were purchased from Strem Chemicals. Aluminum-sec-butoxide (95%), titanium(IV) isopropoxide (95%), pyridine (HPLC grade, 99.5+%), quinoline (98%), indole (99%), thiophene (99%), and benzothiophene (98+%), decahydronaphthalene (98%) were purchased from Alfa Aesar. Naphthalene was purchased from Caledon. Tetraethoxysilane (TEOS) was purchased from Fluka. Ethanol (100%, anhydrous) was purchased from Commercial Alcohol. Millipore water was used throughout. Hydrochloric acid (concentrated) was purchased from EMD. Isopropanol and toluene were purchased from Fischer Scientific. Isopropanol was dried over molecular sieves and stored under argon until used. Toluene was purified through a solvent purification system and was stored under argon until used. Hydrogen, argon, and 5% hydrogen/95% argon were supplied by Praxair.

Instrumentation. A Cavro MSP 9500 Automated Sample Processor purchased from Symyx was used to dispense the substrate solutions into the sample plates. A High Pressure Reactor and Heated Orbital Shaker System (HOSS) purchased from Symyx were used for the reaction testing at a temperature of 22 °C and at an orbital shaking speed of 450 rpm. An Agilent 5975B GC-MS was used to analyze the components of the hydrogenation reaction during the catalyst screening. A Parr

pressure vessel, model 4774-T-SS-3000, and a model 4838 controller with a pressure display module were used to monitor the progress of the bulk hydrogenation reactions. A Varian CP-3800 Gas Chromatograph with a CP-4800 autosampler with a fused silica capillary column and a FID detector was used to analyze the samples of the reaction mixture during the bulk hydrogenation reactions. For the transmission electron microscopy (TEM) analysis, a JEOL JEM-2200FS was used in STEM mode. For X-ray photoelectron spectroscopy (XPS) measurements, a Kratos Analytical, Axis-Ultra instrument was used for the sample analysis. XPS were performed under UHV conditions ($<10^{-8}$ Torr). The catalyst microstructure was analyzed using X-ray diffraction (XRD), which was performed using a Bruker AXS D8 general area detector diffraction system. A Cu Kα radiation source (λ =1.54056 Å) collected the X-ray scans from a sample mounted on a two-axis rotation stage that also allowed for *XYZ* translation.

Bulk Catalyst Synthesis. Catalysts were synthesized based on a previously published procedure.[86] Briefly, 0.133 M metal salt solutions in ethanol and a 1.788 M aluminum sec-butoxide solution in dichloromethane were prepared. A solution consisting of 20.0 mL of ethanol, 0.260 mL of concentrated hydrochloric acid, and 1.42 mL of Millipore water was also prepared. A 0.375 mL portion of each of the metal salt solutions (for a 50:50 ratio of the two metals for a total metal loading of 1%) was added to a 100 mL polypropylene beaker followed by the following amounts of ethanol, 1.788 M aluminum sec-butoxide, titanium(IV) isopropoxide, tetraethoxysilane (TEOS), and after stirring for 5 min, EtOH/HCl/H$_2$O, depending on the desired composition of the support material (See Supporting Information, Table S1).

Each solution was allowed to age and dry overnight in laboratory ambient conditions. Once completely dry, all catalysts were calcined in air in a tube furnace using the following program: heat to 65 °C (rate 1 °C/min), hold at 65 °C for 30 min, heat to 250 °C (rate 1 °C/min), hold at 250 °C for 3 h, cool to 25 °C (rate 1 °C/min). Then the catalyst was hydrogen annealed under a 5% H$_2$/95% Ar atmosphere as follows: heat to 300 °C (rate 5 °C/min), hold at 300 °C for 3 h, cool down to 25 °C rapidly by opening the furnace.
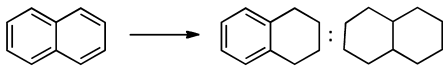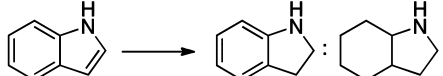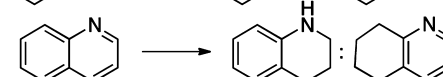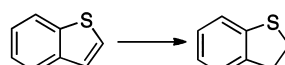
Combinatorial Hydrogenation Screening. Each plate that was tested contained 96 vials, and in each vial 2 × 3 mm borosilicate glass beads were added (Supporting Information, Figure S1). The appropriate amount of catalyst (9−16 mg depending on the composition of the catalyst) was manually weighed into each vial to an accuracy of ±0.4 mg. After each vial contained the appropriate amount of catalyst, the plate was placed into a Cavro MSP 9500 Automated Sample Processor. 0.38 M substrate solutions in isopropanol were prepared in 20 mL vials, and these vials were also loaded into the sample processor. The sample processer was then programmed to dispense 0.4 mL of the appropriate substrate solution into each vial. Once all of the substrate solutions were dispensed, the plate was removed from the sample processer, and was sealed with a top metal plate consisting of a Teflon sheet with a hole above each vial, a silicon sheet with a hole above each vial, and a metal plate with one-way check values (Supporting Information, Figure S2). The top plate was then screwed down securely, and the plate was then encased in a batch reactor (Supporting Information, Figure S3). The batch reactor was then leak tested by pressurizing with nitrogen and monitoring the pressure for several minutes. If there was no change in pressure, then the nitrogen gas was vented, and the batch

reactor was purged with hydrogen three times by slowly pressurizing the batch reactor to the desired pressure, and then slowly depressurizing it. After purging, the batch reactor was pressurized a final time, and then sealed. The batch reactor was disconnected from the gas line and loaded into the HOSS (Supporting Information, Figure S4). The HOSS was then programmed to operate at 22 °C at 450 rpm for the allotted amount of time. After the allotted amount of time, the HOSS was stopped, and the batch reactor was removed, and depressurized very slowly. The batch reactor was then disassembled, the plate was removed from the batch reactor, and the vials were transferred into a different plate for analysis. The analysis plate was then sealed with a top plate consisting of a solid Teflon sheet, a solid rubber sheet, and then the top metal plate that had holes directly above each vial (Supporting Information, Figure S5). The top plate was then screwed down securely to prevent cross-contamination from the other vials. This plate was then loaded into the GC-MS for analysis.

Bulk Hydrogenation: Naphthalene Pressure and Temperatures Studies, Quinoline Pressure Study, and Quinoline Loading Study. The appropriate amount of catalyst to give 3.8×10^{-5} mol of metal was weighed into a 20 mL glass beaker, and a glass coated stir bar was added. Then either a 0.38 M solution of naphthalene in isopropanol was prepared, and 10.0 mL of this solution was added to the beaker, or 10.0 mL of isopropanol followed by the appropriate amount of quinoline (e.g., 0.45 mL for a 100× molar excess of substrate) was added to the beaker containing the catalyst. The beaker was then placed into the bottom of the Parr reactor with the gas inlet in the reaction solution (and the temperature thermocouple for the temperature studies). The Parr reactor was assembled, and the reactor was purged 3 times with H$_2$ by pressurizing followed by venting of the H$_2$ gas. The reactor was then pressurized to the desired pressure, (and allowed to come to the set temperature for the temperature studies) the recorder program was started, and the speed of the stir plate was set. The pressure of the reaction was monitored for a minimum of 7 h for the temperature, pressure, and combination studies, or until the decrease in pressure was <1 psi/hour for the quinoline loading studies. At the end of each hydrogenation reaction, the reactor was disassembled, and a sample of the reaction mixture was analyzed by gas chromatography to determine the hydrogenation products. For the quinoline loading study, the Parr reactor was repressurized as needed because the volume of hydrogen required to completely hydrogenate the quantity of substrate used exceeded that of the Parr reactor at the initial pressure of the reactor. The observed (initial) rates were calculated using the first 2 h of collected data.

Bulk Hydrogenation: Quinoline Temperature Study. An appropriate amount of catalyst to give 3.8×10^{-5} mol of metal was weighed into a 3-neck round-bottom flask. A glass coated stir bar was added to the flask, and then a reflux condenser was added to the middle neck of the round-bottom flask. A gas adapter was attached to the top of the reflux condenser, and the other two necks on the round-bottom flask were sealed with septa. The round-bottom flask was then placed into an oil bath that had been heated to the desired temperature. The flask and reflux condenser were then purged with Ar by placing the entire apparatus under vacuum, and then backfilling it with Ar. This was repeated twice more, and then 10.0 mL of isopropanol were transferred into the round-bottom flask. Then the flask and reflux condenser were purged with hydrogen by briefly placing the entire apparatus under vacuum

Table 1. Screening Hydrogenation Results and Product Distribution using Select Catalysts

Substrates and Products	Catalysts[a]		
	Rh_1/Al_2O_3	$Rh_{0.5}Pt_{0.5}/Al_2O_3$	$Rh_{0.33}Pt_{0.33}Ir_{0.33}/Al_2O_3$
(toluene → methylcyclohexane)	40	39	43
(naphthalene → tetralin : decalin)	8:Trace	7:Trace	6:Trace
(indole → indoline : octahydroindole)	8:10	6:6	6:6
(quinoline → tetrahydroquinoline : 5,6,7,8-tetrahydroquinoline)	58:Trace	65:1	53:Trace
(benzothiophene → 2,3-dihydrobenzothiophene)	3	3	3

[a]Values given as percent product observed as product by GC-MS after 24 h stirring at 150 psi H_2.

and then backfilling it with H_2. This was repeated a total of 5 times. Next 0.59 mL (3.8×10^{-3} mol) of decahydronaphthalene (internal standard) and 0.45 mL (3.8×10^{-3} mol) of quinoline were added via syringe. The reaction was monitored every 15 min for the first 2 h, and then every hour for an additional 5 h. To measure the progress of the hydrogenation reaction 0.2 mL portions were removed from the reaction mixture, and were filtered into a GC vial for analysis. Then 1.0 mL of dichloromethane was run through the used filter into the same GC vial, and finally an additional 0.5 mL of dichloromethane was added to the GC vial. The observed (initial) rates were calculated using the first 2 h of collected data.

Sample Preparation for XPS, TEM, and XRD. XPS: The dried samples were first finely ground to reduce particle size. The ground powders were then placed into a die and pressed into a pellet under high pressure. The pellet was then used for XPS analysis. TEM (before hydrogenation): Raw samples were carefully ground with a mortar and pestle for 20 min. The average particle size is less than 100 nm after being ground. A small amount of the ground powder was then mounted on a carbon-coated grid for TEM analysis. XRD: The samples were prepared by grinding into a fine powder using a mortar and pestle, then pressed into a pellet and mounted on a piece of (100) silicon.

RESULTS AND DISCUSSION

In the development of the catalyst library and screening, three different variables were examined, including metal NP composition, oxide support composition, and the choice of organic aromatic substrates. Starting with the metal NP precursor composition, 4 different metals were utilized, Rh, Pt, Ir, and Ru, to produce six unique NP compositions (Rh, RhPt, RhIr, RuPt, IrPt, and RhPtIr). Of the many possible trimetallic combinations, RhPtIr supported on Al_2O_3 was chosen based on preliminary screening of toluene hydrogenation, as was carried out in previous related work;[86] the results are summarized in Supporting Information, Figure S6.

For each different catalyst composition, the molar ratio of metal to metal oxide was constant at one percent, and for the multimetallic NP systems, the quantities of the different metals comprising the NPs always totaled one percent in equal ratios.

Because of the importance of the nature of the oxide support, 3 different oxide precursor materials were used to produce 12 different supports (pure Al_2O_3, SiO_2, and TiO_2, and 9 binary combinations). The activities of the catalysts were challenged against 7 aromatic substrates, 5 of which were polyaromatic, two were monoaromatic (toluene and thiophene), and 5 contained N or S-heteroatoms. The aromatic substrates screened for hydrogenation are shown in Scheme 1.

The approach used to synthesize the catalysts has been described previously,[86] and is based upon a one-pot approach in which the metal chloride salts (destined to become the metallic NPs), the water sensitive metal alkoxides (the precursors for the oxide support), and an ethanol/water/hydrochloric acid solution were mixed together.[98,113,114] To modify the composition of the catalyst support, the ratios of the different metal alkoxides (and subsequently the amount of solvent, water, and hydrochloric acid) were varied according to the desired composition. An acid catalyzed sol−gel synthesis route was chosen and applied throughout because it allowed for the flexibility of using different water sensitive metal alkoxides without requiring modification of the synthesis procedure. Additionally, when synthesizing mixed metal oxides, precipitation and phase separation of one metal oxide during the sol−gel synthesis can be avoided when using an acid as a catalyst.[115,116]

Initially, all 72 catalysts were screened for the hydrogenation of toluene, naphthalene, pyridine, indole, quinoline, thiophene and benzothiophene at a pressure of 75 psi H_2 (∼5 atm) for a period of 4 h using a Symyx heated orbital shaker system.

Upon subsequent analysis of the reaction mixtures by GC-MS, some degree of catalytic activity was detected for the hydrogenation of toluene, naphthalene, indole, quinoline and benzothiophene, but no hydrogenation was observed for either pyridine or thiophene using any of the 72 NP catalysts. Because the hydrogenation of toluene had already been examined in detail with catalyst libraries prepared in the same manner,[86] it was used as a control reaction against which new catalysts were compared. While hydrogenation of thiophene is difficult,[91] there has been previous success with the hydrogenation of pyridine.[17,91] In addition, 16 of the 72 screened catalysts were observed to be inactive for all of the substrates examined. The

inactive catalysts were those supported on SiO_2, $SiO_2(50\%)-TiO_2(50\%)$, and $SiO_2(25\%)-TiO_2(75\%)$.

The 56 catalysts of the original 72 that demonstrated some activity were tested at a higher pressure of 150 psi H_2 for 24 h, and the reaction mixtures were once again analyzed by GC-MS; the highest catalytic activities for three active metal NP systems and five substrates are shown in Table 1 as an example. A visualization approach for presentation of the data was chosen to allow for easier identification of active catalysts and trends, with the results shown in Figure 1 for toluene, naphthalene, indole, and quinoline; the benzothiophene results are shown in the Supporting Information, Figure S7. For toluene and quinoline, the trend is clear: the metal combination is relatively unimportant as most combinations of these three metals are active for a given metal oxide. The support composition, however, plays an important role with pure Al_2O_3 or Al_2O_3-containing supports leading generally to higher activities. With naphthalene and indole, in particular, the results show more scatter as both the metal and the support compositions have obvious significant effects on activity.

Of all the substrates examined, quinoline was the most active. The observed percent hydrogenation values exceeded those observed for the hydrogenation of any of the substrates examined. Surprisingly, the hydrocarbon analogue of quinoline, naphthalene, did not exhibit comparable percent hydrogenation values, suggesting that the nitrogen heteroatom in the aromatic ring renders the molecule more susceptible to catalytic hydrogenation. The only product observed for the hydrogenation of quinoline under these conditions was the partially hydrogenated 1,2,3,4-tetrahydroquinoline. The fully hydrogenated decahydroquinoline typically requires much harsher conditions (temperatures in the rate of 175−280 °C, hydrogen pressure between 109 and 207 atm H_2 and an acidic solvent) for complete hydrogenation.[118] Quinoline hydrogenation with these metal NPs works best on a full Al_2O_3 support, or a blend containing higher amounts of Al_2O_3 when compared to SiO_2 and TiO_2 (Figure 1d).

Once the 72 different NP catalysts had been screened for activity for the hydrogenation of toluene, naphthalene, pyridine, indole, quinoline, thiophene, and benzothiophene, several catalysts and substrates were selected for further studies in bulk format. $Rh_{0.5}Pt_{0.5}/Al_2O_3$ was chosen because it was the most active bimetallic catalyst. Rh_1/Al_2O_3 and $Rh_1/Al_2O_3(25\%)$-$SiO_2(75\%)$ were selected because they were active for the hydrogenation of naphthalene, and their inclusion in the bulk studies would allow for the effects of a mixed metal oxide support to be explored. $Rh_{0.33}Pt_{0.33}Ir_{0.33}/Al_2O_3$ was chosen because it was the most active trimetallic NP catalyst, and 0.5% Rh/Al_2O_3 because it is a commercially available catalyst. Two substrates were chosen for further studies: naphthalene and quinoline, to compare and contrast the effect of the nitrogen heteroatom. To measure the naphthalene and quinoline hydrogenation rates in bulk, a pressure reactor was used, and the decrease in hydrogen pressure was monitored as a function of time. The observed rates were calculated using the first 2 h of the hydrogenation data, though at least 7 h of data were collected, and at the end of the reaction a sample of the reaction mixture was analyzed by GC to determine the product distribution and to confirm that the decrease in hydrogen pressure was due to catalytic hydrogenation. The rates were measured at initial pressures of 74 psig (∼5 atm), 147 psig (∼10 atm), 294 psig (∼20 atm), and 441 psig (∼30 atm) at ambient temperatures using five different catalysts.

Figure 1. Toluene (a), naphthalene (b), indole (c), and quinoline (d) hydrogenation results. The percent hydrogenation was measured after 24 h of stirring at 150 psi hydrogen pressure. Methylcyclohexane was the exclusive product observed for the hydrogenation of toluene, tetralin, and decalin for the hydrogenation of naphthalene, 2,3-dihydroindole for the hydrogenation of indole, and 1,2,3,4-tetrahydroquinoline for the hydrogenation of quinoline.

Quinoline hydrogenation in bulk, using Al_2O_3 or Al_2O_3-blend catalysts, showed moderate rates at lower pressures, as shown

in Figure 2a. When the hydrogenation of quinoline was investigated under several different initial pressures, only the
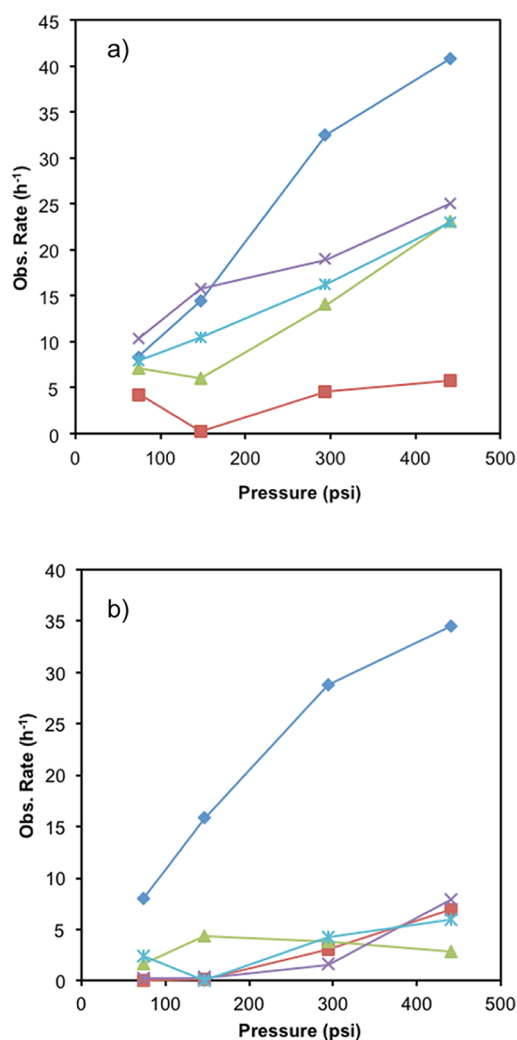

Figure 2. Observed initial rates for the hydrogenation of quinoline (a) and naphthalene (b) at room temperature and various pressures using select catalysts. Blue: commercial 0.5% Rh/Al_2O_3 catalyst. Red: $Rh_1/Al_2O_3(25\%)$-$SiO_2(75\%)$ catalyst. Green: Rh_1/Al_2O_3 catalyst. Purple: $Rh_{0.5}Pt_{0.5}/Al_2O_3$ catalyst. Turquoise: $Rh_{0.33}Pt_{0.33}Ir_{0.33}/Al_2O_3$.

partially hydrogenated product, 1,2,3,4-tetrahydroquinoline, was detected. At lower pressures (74 and 147 psig), the $Rh_{0.5}Pt_{0.5}/Al_2O_3$ catalyst was the most active catalyst, followed closely by the commercial 0.5% Rh/Al_2O_3 and then the $Rh_{0.33}Pt_{0.33}Ir_{0.33}/Al_2O_3$ catalyst. At higher pressures (294 and 441 psig), however, the commercial 0.5% Rh/Al_2O_3 catalyst was the most active, followed by the bimetallic $Rh_{0.5}Pt_{0.5}/Al_2O_3$ catalyst and the trimetallic $Rh_{0.33}Pt_{0.33}Ir_{0.33}/Al_2O_3$ catalyst. Naphthalene hydrogenation (Figure 2b), on the other hand, was poor, with the commercial Rh catalyst far outperforming the sol–gel Rh or mixed metal catalysts.

The effect of temperature on the hydrogenation of quinoline was examined at constant pressure (1 atm H_2), using several catalysts (Figure 3). The commercial 0.5% Rh/Al_2O_3 and $Rh_{0.5}Pt_{0.5}/Al_2O_3$ catalysts demonstrated very similar catalytic activities at all of the temperatures investigated. The sol–gel prepared monometallic Rh_1/Al_2O_3 catalyst showed an increase in catalytic activity as the temperature was increased to 60 °C.
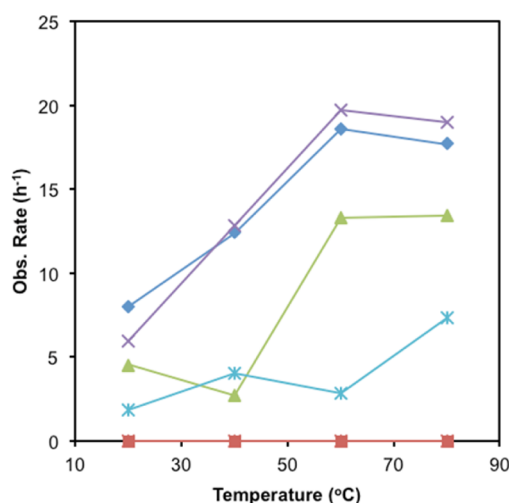
Figure 3. Observed initial rates for the hydrogenation of quinoline at 1 atm H_2 and various temperatures using select catalysts. Blue: commercial 0.5% Rh/Al_2O_3 catalyst. Red: $Rh_1/Al_2O_3(25\%)$-$SiO_2(75\%)$ catalyst. Green: Rh_1/Al_2O_3 catalyst. Purple: $Rh_{0.5}Pt_{0.5}/Al_2O_3$ catalyst. Turquoise: $Rh_{0.33}Pt_{0.33}Ir_{0.33}/Al_2O_3$.

The trimetallic $Rh_{0.33}Pt_{0.33}Ir_{0.33}/Al_2O_3$ catalyst, on the other hand, showed only moderate activities over this temperature range. Finally, the $Rh_1/Al_2O_3(25\%)$-$SiO_2(75\%)$ catalyst was inactive at 1 atm H_2 at all temperatures. For naphthalene, the commercial Rh catalyst far outperformed any of the sol–gel NP catalysts (Supporting Information, Figure S8).

A quinoline loading study was performed where the ratio of quinoline to metal in the catalyst was varied to include ratios of 200, 500, and 1000 in isopropanol (Figure 4), as well as neat (liquid) quinoline (Table 2 and Figure 5). At the original quinoline loading of 100, the commercial 0.5% Rh/Al_2O_3 catalyst was the most active with the other catalysts exhibiting similar catalytic activities, but at loading ratios of 200 and 500,
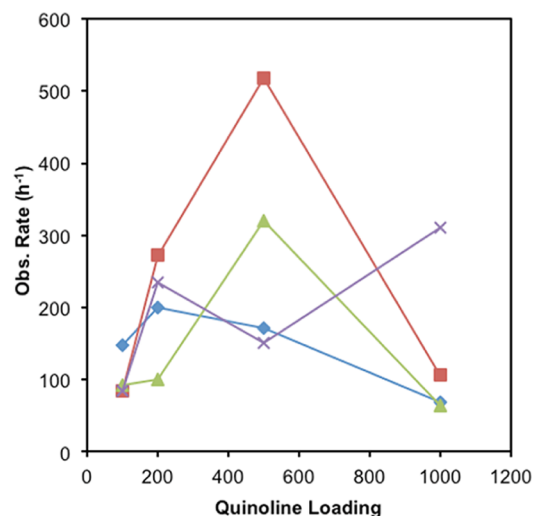

Figure 4. Quinoline loading study using select catalysts. Observed initial rate given as mol of H_2 consumed per mol of metal in catalyst per hour. The reactions were run at 30 atm H_2, and either 60 or 80 °C depending on which temperature would yield the highest catalytic activity for a given catalyst. Blue: commercial 0.5% Rh/Al_2O_3 catalyst. Red: Rh_1/Al_2O_3 catalyst. Green: $Rh_{0.5}Pt_{0.5}/Al_2O_3$ catalyst. Purple: $Rh_{0.33}Pt_{0.33}Ir_{0.33}/Al_2O_3$ catalyst.

Table 2. Neat Quinoline Hydrogenation Results using Select Catalysts[a]

catalyst	obs. rate $(h^{-1})^{b}$	time (h)	% quin	% THQ
comm. 0.5% Rh	214	115	27.1	72.9
Rh_1	205	93	28.7	71.3
$Rh_{0.5}Pt_{0.5}$	141	145	29.5	70.5
$Rh_{0.33}Pt_{0.33}Ir_{0.33}$	69	156	28.2	71.8

[a]Reaction conditions: 30 atm H_2, 60 or 80 °C, no solvent, 3.8×10^{-5} mol metal, substrate/cat. = 2000:1 = 0.076 mol quinoline. All catalysts were supported on Al_2O_3. THQ = 1,2,3,4-tetrahydoquinoline. Because the molar amount of hydrogen contained in the Parr reactor at an initial pressure of 30 atm was less that that required to completely hydrogenate quinoline, hydrogen was added as needed by repressurizing the Parr reactor to 30 atm. [b]Observed initial rate given as mol of hydrogen consumed per hour, and was measured using the first 2 h of hydrogen consumption data.
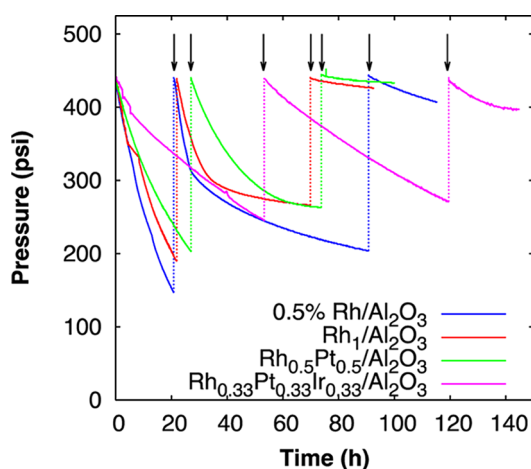
Figure 5. Kinetic results for the neat hydrogenation of quinoline using select catalysts. The sharp increases in pressure as indicated by the dashed lines and arrows were due to the pressure chamber being repressurized to ensure that the amount of hydrogen was not rate limiting. Reaction conditions: 30 atm H_2, 60 or 80 °C, no solvent, 3.8×10^{-5} mol metal, substrate/cat. = 2000:1 = 0.076 mol quinoline.

the activities of both Rh_1/Al_2O_3 and $Rh_{0.5}Pt_{0.5}/Al_2O_3$ increased. Overall, the Rh_1/Al_2O_3 catalyst was the most active with an observed rate of 519 h^{-1} at a loading ratio of 500. At the higher loading ratio of 1000, the activity of the Rh_1/Al_2O_3 and $Rh_{0.5}Pt_{0.5}/Al_2O_3$ catalysts substantially decreased whereas the trimetallic $Rh_{0.33}Pt_{0.33}Ir_{0.33}/Al_2O_3$ catalyst was over 3 times more active than any of the other tested catalysts. With an observed rate of 310 h^{-1}, this rate was the highest overall activity obtained for the trimetallic catalyst. With the exception of the trimetallic catalyst at this loading ratio, substrate inhibition is evident at higher quinoline loading ratios. The notable differences in catalytic activity between the commercial 0.5% Rh/Al_2O_3 catalyst and the synthesized Rh_1/Al_2O_3 catalyst may be attributed to the different synthetic methods used to prepare them. The commercial catalyst was synthesized using the traditional impregnation or incipient wetness route where the prefabricated metal oxide was soaked in solution of the metal NP precursor followed by reduction of the metal NP precursor. The catalysts described here were prepared by first synthesizing the metal oxide with the accompanying metal NP precursor, followed by reduction of the metal NP precursor to NPs. Our earlier results also show that the average size of the NPs in the commercial catalyst is 5.2 nm whereas the average

size of the NPs in the synthesized Rh_1/Al_2O_3 catalyst is 2.6 nm (Supporting Information, Figure S9b). The different synthesis methods in conjunction with the different NP sizes indicate that the two Rh/Al_2O_3 catalysts, while compositionally similar, possess different catalytic activities.

The neat hydrogenation of quinoline using the same catalysts was successful, with the results shown in Table 2 and Figure 5. Because the quantity of hydrogen required to fully hydrogenate the amount of quinoline used in the neat hydrogenation studies exceeded that contained within the Parr reactor at an initial pressure of 30 atm, hydrogen was added as needed by repressurizing the Parr reactor to 30 atm as indicated by the dashed lines and arrows in Figure 5. It was observed that all of the studied catalysts were active for this reaction and that 1,2,3,4-tetrahydroquinoline was the only product detected at the end of the reaction by GC (Table 2). Considering the results for the first 20 h of the reaction, as can be seen in Figure 5, the most active catalyst was the commercial Rh catalyst, followed by the sol−gel prepared monometallic Rh catalyst, the bimetallic catalyst, and the trimetallic catalyst, respectively. In terms of longevity, it appears that the commercial catalyst and the trimetallic catalyst maintain their activity. Overall, the commercial catalyst was most active at the beginning of the reaction, and both the commercial and the trimetallic catalysts show no significant decrease in activity throughout the 100−120 h reaction time whereas the monometallic Rh and bimetallic RhPt catalysts become deactivated at an earlier point in the reaction. The observed decrease in rate was due to a decrease in the quantity of hydrogen available, and not due to irreversible deactivation of the catalysts themself. Once the reaction vessel was repressurized, the monometallic Rh and bimetallic RhPt catalysts exhibited a catalytic activity comparable to that observed at the beginning of the reaction.

The synthetic approach taken here to produce, in a simultaneous fashion, the NPs and the oxide support, does not attempt to directly control NP size. It is, therefore, important to obtain a better understanding of NP size distributions, and other characteristics, to evaluate any relationship with catalytic activity. It was demonstrated that support composition had an important influence on catalytic performance, with silica supports leading to the lowest catalytic activity. NP catalysts supported on SiO_2 were determined by TEM to be larger than those supported on Al_2O_3 or TiO_2 (Table 3). These results suggest that when the same synthesis method is used to prepare NP catalysts on different metal oxide support materials, the support composition affects the resulting size of the NPs. The size of the NPs has a direct affect on their catalytic activity, in addition to the known influence of support composition, pretreatment, and other parameters.[19,68,69,117] In the case of titania, TiO_2 supported NPs may be less active because of a strong metal support interaction (SMSI).[68]

Because the $Rh_1/Al_2O_3(25\%)$-$SiO_2(75\%)$ catalyst generally underperformed the commercial 0.5% Rh/Al_2O_3 catalyst for the hydrogenation of naphthalene and quinoline, TEM and XPS were carried out, before hydrogenation, to determine if there was an obvious difference in NP size and oxidation state for this pair of catalysts, and the results are summarized in Table 3. Because of the similar oxidation state of the commercial 0.5% Rh/Al_2O_3 catalyst when compared to the $Rh_1/Al_2O_3(25\%)$-$SiO_2(75\%)$ catalyst and the similar NP size of the $Rh_1/Al_2O_3(25\%)$-$SiO_2(75\%)$ (Figure 6) to the other active catalysts, it suggests that the low catalytic activity of $Rh_1/Al_2O_3(25\%)$-$SiO_2(75\%)$ for hydrogenation of naphthalene and quinoline is

Table 3. Summary of Pre-Catalysis TEM and XPS Results

catalyst	NP diameter (nm)		BE (eV)		
Rh_1/SiO_2	5.2 ± 1.6	Figure S9a	307.4		Figure S14
Rh_1/Al_2O_3	2.6 ± 0.5	Figure S9b	308.0		Figure S13
Rh_1/TiO_2	2.2 ± 0.7	Figure S9c	N/A		
0.5% $Rh/Al_2O_3^a$	5.2 ± 1.6	ref 86.	308.8		ref 86.
$Rh_1/Al_2O_3(25\%)$-$SiO_2(75\%)$	2.7 ± 0.7	Figure 6	308.7		Figure S10
$Rh_{0.5}Pt_{0.5}/Al_2O_3^b$	3.1 ± 1.0	ref 86.	306.7 (Rh), 71.4 (Pt)		ref 86.
$Rh_{0.33}Pt_{0.33}Ir_{0.33}/Al_2O_3$	2.7 ± 0.6	Figure S11	306.9 (Rh), 71.4 (Pt), 60.7 (Ir)		Figure S11

^{a}The TEM images and XPS spectrum for 0.5% Rh/Al_2O_3 were previously published in ref 86 as Figure 4e and Supporting Information, Figures S9. ^{b}The TEM images and XPS spectra for $Rh_{0.5}Pt_{0.5}/Al_2O_3$ were previously published in ref 86 as Figures 4a, 6, and 7.
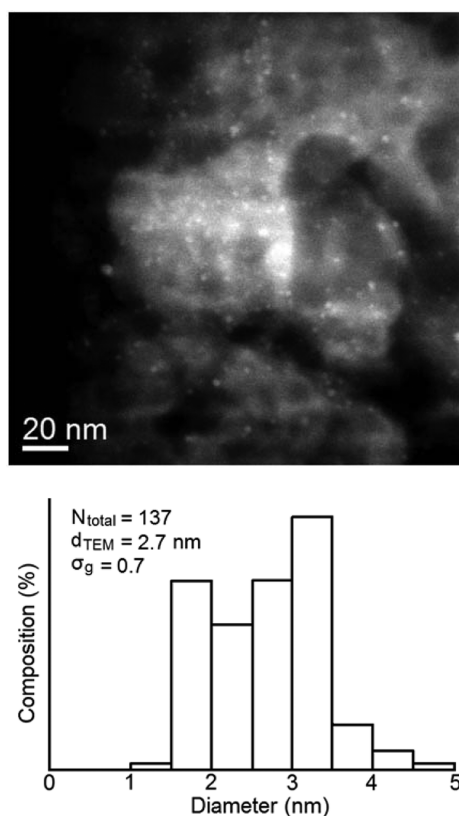
Figure 6. Precatalysis TEM image and particle size histogram for $Rh_1/Al_2O_3(25\%)$-$SiO_2(75\%)$.

due to other factors, such as interactions between the metal and the support. It should also be noted that the oxidation state of the active NP catalysts during catalysis may differ from those noted here, since XPS is an ex situ, high vacuum characterization method.

There are a number of ways to study the metal–support interaction between metal NPs and a metal oxide support including extended X-ray absorption fine structure (EXAFS) and XPS.[27,119−121] XPS can establish an electronic interaction between the metal NPs and the metal oxide support by observing shifts in the binding energy (BE) of the metal of interest.[120,121] Electron donation from the metal NPs to the

metal oxide support would manifest itself as a shift of the BE to higher values, but oxidation of the NPs will also lead to the same result.[27] In contrast, if electron donation from the metal oxide support to the metal NP is occurring, the BE values will shift to lower values.[119] Considering the XPS spectra of our catalysts, none of the metal NPs have a shift in their BE to lower values with respect to their zero oxidation state BE, indicating that electron donation from the metal oxide support to the metal NP is not occurring. The metal NPs in $Rh_{0.5}Pt_{0.5}/Al_2O_3$ and $Rh_{0.33}Pt_{0.33}Ir_{0.33}/Al_2O_3$ all appear to be in zero oxidation states (Table 3) whereas the metal NPs in the Rh_1/Al_2O_3, $Rh_1/Al_2O_3(25\%)$-$SiO_2(75\%)$, and Rh_1/SiO_2 catalysts all have their Rh BEs shifted to higher values with the largest shift observed for mixed metal oxide supported catalyst; whether this increase is due to NP surface oxidation or electron withdrawal by the support cannot be determined. It is known that aromatic hydrogenation with supported metal NP catalysts is complicated by pretreatment effects, differences of surface composition and other factors.[19,69,117] It is difficult at this stage to reach any broad conclusions as to the nature of the metal–support interaction.

XRD was carried out to determine the structure of the supported NP samples. We prepared and attempted to characterize Rh_1/Al_2O_3 by XRD (as shown in the Supporting Information, Figure S15), but because a significant portion of the Al_2O_3 is crystalline, the diffracted intensity from the crystalline Al_2O_3 overwhelms the small amount of signal from the Rh NPs. However, when the same metal NPs were prepared on SiO_2, crystalline FCC Rh NPs were clearly identifiable as the SiO_2 support is amorphous. The (111), (200), and (220) Rh peaks are visible, as shown in Figure 7,
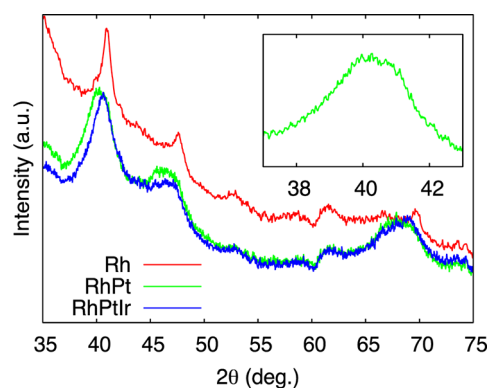
Figure 7. XRD patterns of Rh_1/SiO_2, $Rh_{0.5}Pt_{0.5}/SiO_2$, and $Rh_{0.33}Pt_{0.33}Ir_{0.33}/SiO_2$. The inset shows a close up of the $Rh_{0.5}Pt_{0.5}/SiO_2$ XRD pattern highlighting the distinctly non-Lorentzian profile, suggesting that this peak may be the superposition of the peaks from two separate FCC phases with similar lattice parameters.

from which a lattice parameter of 3.820 ± 0.001 A is determined, agreeing well with the literature value of 3.82000 A [JCPDS 01-071-4657]. The average size of the Rh NPs was determined to be 4.5 ± 0.9 nm as measured by the Scherrer equation. These grain sizes agree well with those of the NPs as determined by TEM (Table 3, Supporting Information, Figure S9a).

By comparing the XRD spectra obtained for Rh_1/SiO_2 to those obtained for $Rh_{0.5}Pt_{0.5}/SiO_2$ and $Rh_{0.33}Pt_{0.33}Ir_{0.33}/SiO_2$, it can be seen that all three samples have different metallic phases (Figure 7). Close inspection of the RhPt XRD pattern reveals that the three strongest reflections have a distinctly non-

Lorentzian profile, where the peak curvature is anomalously low (i.e., the peaks appear to be "flattened" at the top). This result suggests that these peaks may be the superposition of features from two separate FCC phases with similar lattice parameters. By curve fitting each of the peaks at the sum of two separate reflections, the extracted lattice parameters of these FCC phases are 3.82 ± 0.02 and 3.92 ± 0.02 A. These values agree well with the literature values of Rh and Pt (3.8034 and 3.91610 A, respectively) [JCPDS 01-071-4657 and JCPDS 00-001-1194]. This two phase mixture of FCC Rh and Pt is substantiated by the binary phase diagram,[122] where a large miscibility gap is observed at temperatures below ∼760 °C. From the Scherrer equation, the grain size for Pt NPs was found to be 2.2 ± 0.8 nm and 4.0 ± 1.0 nm for Rh NPs (Supporting Information, Figure S16).

With regards to the $Rh_{0.33}Pt_{0.33}Ir_{0.33}/SiO_2$ sample, it appears that a single FCC metal phase is present based on the peak shape. Unlike the $Rh_{0.5}Pt_{0.5}/SiO_2$ sample, each of the primary reflections from $Rh_{0.33}Pt_{0.33}Ir_{0.33}/SiO_2$ XRD scan are well fit by a single Lorentzian profile. These reflections can be matched to a single FCC phase with a lattice parameter of 3.847 ± 0.002, and from the Scherrer equation the grain size was measured to be 2.8 ± 0.3 nm.

These XRD results shed some new light on some of the trends that were observed for the catalytic activity of our catalysts at higher quinoline loadings. Since the XRD results suggest that the $Rh_{0.5}Pt_{0.5}$ catalyst is composed of individual Rh and Pt NPs, and from previous work it was found that our Pt catalysts were inactive for aromatic hydrogenation,[86] we can conclude that by incorporating Pt into the Rh catalyst, we have simply decreased the amount of catalytically active Rh. This result provides a possible explanation as to why the trends of Rh_1/Al_2O_3 and $Rh_{0.5}Pt_{0.5}/Al_2O_3$ in Figure 4 are so similar, with the catalytic activity of $Rh_{0.5}Pt_{0.5}/Al_2O_3$ being approximately half of that for Rh_1/Al_2O_3; there is half as much catalytically active metal in the binary case. The XRD results suggest an explanation for the differences in catalytic activity observed with the ternary system, $Rh_{0.33}Pt_{0.33}Ir_{0.33}/Al_2O_3$. Because the XRD patterns indicate that the trimetallic catalyst is a disordered substitutional solid solution alloy as opposed to individual Rh, Pt, and Ir NPs, it would be expected that this catalyst would exhibit a unique catalytic behavior when compared to the monometallic Rh_1/Al_2O_3 and the bimetallic $Rh_{0.5}Pt_{0.5}/Al_2O_3$ catalysts. Highly detailed TEM and/or synchrotron studies would be required to fully elucidate the nature of the trimetallic versus bimetallic catalyst systems.

CONCLUSIONS

In this work 72 different heterogeneous NP catalysts were efficiently screened for the hydrogenation of toluene, naphthalene, pyridine, indole, quinoline, thiophene, and benzothiophene under mild conditions by using a combinatorial approach. On the basis of the screening results, several active catalysts were identified and chosen for further studies in bulk for the hydrogenation of naphthalene and quinoline. Naphthalene and quinoline are similar bicyclic molecules, differing only with a nitrogen atom substitution. Using the same bulk catalyst under identical conditions, it was observed that quinoline was the rapidly hydrogenated substrate of the series. The screening also demonstrated that support composition had a large affect on the catalytic activity, even when the size and oxidation state of the NPs on the different supports were comparable. XRD results suggest that discrete monometallic

NP catalysts populations may be formed under some conditions, whereas mixed metal alloy NP catalysts result under other conditions. Because of the enormous number of combinations of binary, ternary, and quarternary mixed metal NP combinations that can be envisaged, this work points to the challenges of identifying new catalyst compositions, and elucidating the reasons for their observed activity.

ASSOCIATED CONTENT

Ⓢ Supporting Information

Table of reagents used and quantities for the synthesis of the metal oxide supports; images of equipment used at CCRI; plots of hydrogenation results for ternary and quaternary metal systems, benzothiophene hydrogenation results, and naphthalene hydrogenation rates; TEM images and NP histograms for Rh_1/SiO_2, Rh_1/Al_2O_3, Rh_1/TiO_2, and $Rh_{0.33}Pt_{0.33}Ir_{0.33}/Al_2O_3$; XPS spectra of $Rh_1/Al_2O_3(25\%)$-$SiO_2(75\%)$, $Rh_{0.33}Pt_{0.33}Ir_{0.33}/Al_2O_3$, Rh_1/Al_2O_3, and Rh_1/SiO_2; XRD patterns of Al_2O_3 and Rh_1/Al_2O_3; XRD curve fitting procedure for $Rh_{0.5}Pt_{0.5}/SiO_2$. This material is available free of charge via the Internet at http://pubs.acs.org.

AUTHOR INFORMATION

Corresponding Author
*E-mail: jburiak@ualberta.ca.

REFERENCES

(1) Strausz, O. P.; Morales-Izquierdo, A.; Kazmi, N.; Montgomery, D. S.; Payzant, J. D.; Safarik, I.; Murgich, J. *Energy Fuels* **2010**, *24*, 5053−5072.

(2) Bukka, K.; Miller, J. D.; Oblad, A. G. *Energy Fuels* **1991**, *5*, 333−340.

(3) Rudzinski, W. E.; Aminabhavi, T. M. *Energy Fuels* **2000**, *14*, 464−475.

(4) Song, C.; Nihonmatsu, T.; Nomura, M. *Ind. Eng. Chem. Res.* **1991**, *30*, 1726−1734.

(5) Beltramone, A. R.; Resasco, D. E.; Alvarez, W. E.; Choudhary, T. V. *Ind. Eng. Chem. Res.* **2008**, *47*, 7161−7166.

(6) Strausz, O. P.; Mojelsky, T. W.; Payzant, J. D.; Olah, G. A.; Prakash, G. K. S. *Energy Fuels* **1999**, *13*, 558−569.

(7) Owusu-Boakye, A.; Dalai, A. K.; Ferdous, D.; Adjaye, J. *Energy Fuels* **2005**, *19*, 1763−1774.

(8) Stanislaus, A.; Cooper, B. H. *Catal. Rev.—Sci. Eng.* **1994**, *36*, 75−123.

(9) Fujikawa, T.; Idei, K.; Ebihara, T.; Mizuguchi, H.; Usui, K. *Appl. Catal., A* **2000**, *192*, 253−261.

(10) Prechtl, M. H. G.; Scariot, M.; Scholten, J. D.; Machado, G.; Teixeira, S. R.; Dupont, J. *Inorg. Chem.* **2008**, *47*, 8995−9001.

(11) Bratlie, K. M.; Lee, H.; Komvopoulos, K.; Yang, P.; Somorjai, G. A. *Nano Lett.* **2007**, 7, 3097−3101.

(12) Hu, L.; Xia, G.; Qu, L.; Li, M.; Li, C.; Xin, Q.; Li, D. *J. Catal.* **2001**, 202, 220−228.

(13) Yang, X.; Yan, N.; Fei, Z.; Crespo-Quesada, R. M.; Laurenczy, G.; Kiwi-Minsker, L.; Kou, Y.; Li, Y.; Dyson, P. J. *Inorg. Chem.* **2008**, 47, 7444−7446.

(14) Kakade, B. A.; Sahoo, S.; Halligudi, S. B.; Pillai, V. K. *J. Phys. Chem. C* **2008**, 112, 13317−13319.

(15) Yoon, B.; Pan, H. B.; Wai, C. M. *J. Phys. Chem. C* **2009**, 113, 1520−1525.

(16) Yoon, B.; Wai, C. M. *J. Am. Chem. Soc.* **2005**, 127, 17174−17175.

(17) Park, I. S.; Kwon, M. S.; Kang, K. Y.; Lee, J. S.; Park, J. *Adv. Synth. Catal.* **2007**, 349, 2039−2047.

(18) Su, F.; Lv, L.; Lee, F. Y.; Liu, T.; Cooper, A. I.; Zhao, X. S. *J. Am. Chem. Soc.* **2007**, 129, 14213−14223.

(19) Lin, S. D.; Vannice, M. A. *J. Catal.* **1993**, 143, 554−562.

(20) Cunha, D. S.; Cruz, G. M. *Appl. Catal., A* **2002**, 236, 55−66.

(21) Mevellec, V.; Nowicki, A.; Roucoux, A.; Dujardin, C.; Granger, P.; Payen, E.; Philippot, K. *New J. Chem.* **2006**, 30, 1214−1219.

(22) Marconi, G.; Pertici, P.; Evangelisti, C.; Caporusso, A. M.; Vitulli, G.; Capannelli, G.; Hoang, M.; Turney, T. W. *J. Organomet. Chem.* **2004**, 689, 639−646.

(23) Spinace, E. V.; Vaz, J. M. *Catal. Commun.* **2003**, 4, 91−96.

(24) Yuan, T.; Fournier, A. R.; Proudlock, R.; Marshall, W. D. *Environ. Sci. Technol.* **2007**, 41, 1983−1988.

(25) Dominguez-Quintero, O.; Martinez, S.; Henriquez, Y.; D'Ornelas, L.; Krentzien, H.; Osuna, J. *J. Mol. Catal. A: Chem.* **2003**, 197, 185−191.

(26) Lang, H. F.; May, R. A.; Iversen, B. L.; Chandler, B. D. *J. Am. Chem. Soc.* **2003**, 125, 14832−14836.

(27) Pawelec, B.; Campos-Martin, J. M.; Cano-Serrano, E.; Navarro, R. M.; Thomas, S.; Fierro, J. L. G. *Environ. Sci. Technol.* **2005**, 39, 3374−3381.

(28) Marecot, P.; Mahoungou, J. R.; Barbier, J. *Appl. Catal., A* **1993**, 101, 143−149.

(29) Zhao, A.; Gates, B. C. *J. Catal.* **1997**, 168, 60−69.

(30) Schulz, J.; Roucoux, A.; Patin, H. *Chem. Commun.* **1999**, 535−536.

(31) Schulz, J.; Roucoux, A.; Patin, H. *Chem.—Eur. J.* **2000**, 6, 618−624.

(32) Deshmukh, R. R.; Lee, J. W.; Shin, U. S.; Lee, J. Y.; Song, C. E. *Angew. Chem., Int. Ed.* **2008**, 47, 8615−8617.

(33) Mu, X. D.; Meng, J. Q.; Li, Z. C.; Kou, Y. *J. Am. Chem. Soc.* **2005**, 127, 9694−9695.

(34) Zhao, C.; Wang, H. Z.; Yan, N.; Xiao, C. X.; Mu, X. D.; Dyson, P. J.; Kou, Y. *J. Catal.* **2007**, 250, 33−40.

(35) Jacinto, M. J.; Kiyohara, P. K.; Masunaga, S. H.; Jardim, R. F.; Rossi, L. M. *Appl. Catal., A* **2008**, 338, 52−57.

(36) Schulz, J.; Levigne, S.; Roucoux, A.; Patin, H. *Adv. Synth. Catal.* **2002**, 344, 266−269.

(37) Harada, T.; Ikeda, S.; Ng, Y. H.; Sakata, T.; Mori, H.; Torimoto, T.; Matsumura, M. *Adv. Func. Mater.* **2008**, 18, 2190−2196.

(38) Zahmakiran, M.; Ozkar, S. *Langmuir* **2008**, 24, 7065−7067.

(39) Zahmakiran, M.; Tonbul, Y.; Ozkar, S. *J. Am. Chem. Soc.* **2010**, 132, 6541−6549.

(40) Hagen, C. M.; Widegren, J. A.; Maitlis, P. M.; Finke, R. G. *J. Am. Chem. Soc.* **2005**, 127, 4423−4432.

(41) Widegren, J. A.; Finke, R. G. *Inorg. Chem.* **2002**, 41, 1558−1572.

(42) Weddle, K. S.; Aiken, J. D.; Finke, R. G. *J. Am. Chem. Soc.* **1998**, 120, 5653−5666.

(43) Leger, B.; Denicourt-Nowicki, A.; Roucoux, A.; Olivier-Bourbigou, H. *Adv. Synth. Catal.* **2008**, 350, 153−159.

(44) Pellegatta, J. L.; Blandy, C.; Colliere, V.; Choukroun, R.; Chaudret, B.; Cheng, P.; Philippot, K. *J. Mol. Catal. A: Chem.* **2002**, 178, 55−61.

(45) Sidhpuria, K. B.; Parikh, P. A.; Bahadur, P.; Jasra, R. V. *Ind. Eng. Chem. Res.* **2008**, 47, 4034−4042.

(46) Simon, L.; van Ommen, J. G.; Jentys, A.; Lercher, J. A. *J. Phys. Chem. B* **2000**, 104, 11644−11649.

(47) Hiyoshi, N.; Rode, C. V.; Sato, O.; Masuda, Y.; Yamaguchi, A.; Shirai, M. *Chem. Lett.* **2008**, 37, 734−735.

(48) Leger, B.; Denicourt-Nowicki, A.; Olivier-Bourbigou, H.; Roucoux, A. *Inorg. Chem.* **2008**, 47, 9090−9096.

(49) Ohde, H.; Ohde, M.; Wai, C. M. *Chem. Commun.* **2004**, 930−931.

(50) Hiyoshi, N.; Inoue, T.; Rode, C.; Sato, O.; Shirai, M. *Catal. Lett.* **2006**, 106, 133−138.

(51) Graydon, W. F.; Langan, M. D. *J. Catal.* **1981**, 69, 180−192.

(52) Zhang, Z. G.; Okada, K.; Yamamoto, M.; Yoshida, T. *Catal. Today* **1998**, 45, 361−366.

(53) Lu, F.; Liu, J.; Xu, H. *Adv. Synth. Catal.* **2006**, 348, 857−861.

(54) Hiyoshi, N.; Osada, M.; Rode, C. V.; Sato, O.; Shirai, M. *Appl. Catal., A* **2007**, 331, 1−7.

(55) Venezia, A. M.; La Parola, V.; Pawelec, B.; Fierro, J. L. G. *Appl. Catal., A* **2004**, 264, 43−51.

(56) Wan, G.; Duan, A.; Zhao, Z.; Jiang, G.; Zhang, D.; Li, R.; Dou, T.; Chung, K. H. *Energy Fuels* **2009**, 23, 81−85.

(57) Thomas, J. M.; Johnson, B. F. G.; Raja, R.; Sankar, G.; Midgley, P. A. *Acc. Chem. Res.* **2003**, 36, 20−30.

(58) Gelman, F.; Avnir, D.; Schumann, H.; Blum, J. *J. Mol. Catal. A: Chem.* **2001**, 171, 191−194.

(59) Pawelec, B.; La Parola, V.; Navarro, R. M.; Murcia-Mascaros, S.; Fierro, J. L. G. *Carbon* **2006**, 44, 84−98.

(60) Roucoux, A.; Schulz, J.; Patin, H. *Chem. Rev.* **2002**, 102, 3757−3778.

(61) Barbaro, P.; Bianchini, C.; Dal Santo, V.; Meli, A.; Moneti, S.; Psaro, R.; Scaffidi, A.; Sordelli, L.; Vizza, F. *J. Am. Chem. Soc.* **2006**, 128, 7065−7076.

(62) Hiyoshi, N.; Miura, R.; Rode, C. V.; Sato, O.; Shirai, M. *Chem. Lett.* **2005**, 34, 424−425.

(63) Barbaro, P.; Bianchini, C.; Dal Santo, V.; Meli, A.; Moneti, S.; Pirovano, C.; Psaro, R.; Sordelli, L.; Vizza, F. *Organometallics* **2008**, 27, 2809−2824.

(64) Roucoux, A. *Top. Organomet. Chem.* **2005**, 16, 261−279.

(65) Liang, C.; Zhao, A.; Zhang, X.; Ma, Z.; Prins, R. *Chem. Commun.* **2009**, 2047−2049.

(66) Gao, H.; Angelici, R. J. *J. Am. Chem. Soc.* **1997**, 119, 6937−6938.

(67) Ioannides, T.; Verykios, X. E. *J. Catal.* **1993**, 143, 175−186.

(68) Crump, C. J.; Gilbertson, J. D.; Chandler, B. D. *Top. Catal.* **2008**, 49, 233−240.

(69) Lin, S. D.; Vannice, M. A. *J. Catal.* **1993**, 143, 539−553.

(70) Takagi, H.; Isoda, T.; Kusakabe, K.; Morooka, S. *Energy Fuels* **1999**, 13, 1191−1196.

(71) Santana, R. C.; Jongpatiwut, S.; Alvarez, W. E.; Resasco, D. E. *Ind. Eng. Chem. Res.* **2005**, 44, 7928−7934.

(72) Pawelec, B.; Castano, P.; Arandes, J. M.; Bilbao, J.; Thomas, S.; Pena, M. A.; Fierro, J. L. G. *Appl. Catal., A* **2007**, 317, 20−33.

(73) Park, K. H.; Jang, K.; Kim, H. J.; Son, S. U. *Angew. Chem., Int. Ed.* **2007**, 46, 1152−1155.

(74) Yang, S. Y.; Stock, L. M. *Energy Fuels* **1998**, 12, 644−648.

(75) Widegren, J. A.; Finke, R. G. *J. Mol. Catal. A: Chem.* **2003**, 191, 187−207.

(76) Pelisson, C.-H.; Vono, L. L. R.; Hubert, C.; Denicourt-Nowicki, A.; Rossi, L. M.; Roucoux, A. *Catal. Today* **2012**, 183, 124−129.

(77) Chen, H.-J.; Liu, H.-W.; Liao, W.; Pan, H. B.; Wai, C. M.; Chiu, K.-H.; Jen, J.-F. *Appl. Catal., B* **2012**, 111−1123, 402−408.

(78) Zahmakiran, M.; Roman-Leshkov, Y.; Zhang, Y. *Langmuir* **2012**, 28, 60−64.

(79) Pan, H. B.; Wai, C. M. *New J. Chem.* **2011**, 35, 1649−1660.

(80) Hubert, C.; Bile, E. G.; Denicourt-Nowicki, A.; Roucoux, A. *Green Chem.* **2011**, 13, 1776−1771.

(81) Bile, E. G.; Sassine, R.; Denicourt-Nowicki, A.; Launay, F.; Roucoux, A. *Dalton Trans.* **2011**, 40, 6524−6531.

(82) Yan, N.; Yuan, Y.; Dyson, P. J. *Chem. Commun.* **2011**, 47, 2559−2531.

(83) Dykeman, R. R.; Yan, N.; Scopelliti, R.; Dyson, P. J. *Inorg. Chem.* **2011**, *50*, 717−719.

(84) Narayanan, R.; El-Sayed, M. A. *J. Phys. Chem. B* **2005**, *109*, 12663−12676.

(85) Yoo, J. W.; Hathcock, D. J.; El-Sayed, M. A. *J. Catal.* **2003**, *214*, 1−7.

(86) Dehm, N. A.; Zhang, X.; Buriak, J. M. *Inorg. Chem.* **2010**, *49*, 2706−2714.

(87) Pan, H. B.; Wai, C. M. *J. Phys. Chem. C* **2009**, *113*, 19782−19788.

(88) Sanchez-Delgado, R. A.; Machalaba, N.; Ng-A-Qui, N. *Catal. Commun.* **2007**, *8*, 2115−2118.

(89) Fang, M.; Machalaba, N.; Sanchez-Delgado, R. A. *Dalton Trans.* **2011**, *40*, 10621−10632.

(90) Grobas, J.; Bolivar, C.; Scott, C. E. *Energy Fuels* **2007**, *21*, 19−22.

(91) Mevellec, V.; Roucoux, A. *Inorg. Chim. Acta* **2004**, *357*, 3099−3103.

(92) Mao, H.; C., C.; Liao, X.; Shi, B. *J. Mol. Catal. A: Chem.* **2011**, *341*, 51−56.

(93) Mott, D.; Luo, J.; Njoki, P. N.; Lin, Y.; Wang, L. Y.; Zhong, C. J. *Catal. Today* **2007**, *122*, 378−385.

(94) Alayoglu, S.; Eichhorn, B. *J. Am. Chem. Soc.* **2008**, *130*, 17479−17486.

(95) Tao, F.; Grass, M. E.; Zhang, Y. W.; Butcher, D. R.; Aksoy, F.; Aloni, S.; Altoe, V.; Alayoglu, S.; Renzas, J. R.; Tsung, C. K.; Zhu, Z. W.; Liu, Z.; Salmeron, M.; Somorjai, G. A. *J. Am. Chem. Soc.* **2010**, *132*, 8697−8703.

(96) Tao, F.; Grass, M. E.; Zhang, Y. W.; Butcher, D. R.; Renzas, J. R.; Liu, Z.; Chung, J. Y.; Mun, B. S.; Salmeron, M.; Somorjai, G. A. *Science* **2008**, *322*, 932−934.

(97) Sun, Y. P.; Chan, B. C.; Ramnarayanan, R.; Leventry, W. M.; Mallouk, T. E.; Bare, S. R.; Willis, R. R. *J. Comb. Chem.* **2002**, *4*, 569−575.

(98) Holzwarth, A.; Schmidt, H. W.; Maier, W. E. *Angew. Chem., Int. Ed.* **1998**, *37*, 2644−2647.

(99) Xiang, X. D.; Sun, X.; Briceno, G.; Lou, Y.; Wang, K. A.; Chang, H.; Wallace-Freedman, W. G.; Chen, S. W.; Schultz, P. G. *Science* **1995**, *268*, 1738−1740.

(100) Briceno, G.; Chang, H.; Sun, X.; Schultz, P. G.; Xiang, X. D. *Science* **1995**, *270*, 273−275.

(101) Wang, J.; Yoo, Y.; Gao, C.; Takeuchi, I.; Sun, X.; Chang, H.; Xiang, X.-D.; Schultz, P. G. *Science* **1998**, *279*, 1712−1715.

(102) Danielson, E.; Devenney, M.; Giaquinta, D. M.; Golden, J. H.; Haushalter, R. C.; McFarland, E. W.; Poojary, D. M.; Reaves, C. M.; Weinberg, W. H.; Wu, X. D. *Science* **1998**, *279*, 837−840.

(103) Danielson, E.; Golden, J. H.; McFarland, E. W.; Reaves, C. M.; Weinberg, W. H.; Wu, X. D. *Nature* **1997**, *389*, 944−948.

(104) Moates, F. C.; Somani, M.; Annamalai, J.; Richardson, J. T.; Luss, D.; Willson, R. C. *Ind. Eng. Chem. Res.* **1996**, *35*, 4801−4803.

(105) Orschel, M.; Klein, J.; Schmidt, H. W.; Maier, W. F. *Angew. Chem., Int. Ed.* **1999**, *38*, 2791−2794.

(106) Woodhouse, M.; Parkinson, B. A. *Chem. Mater.* **2008**, *20*, 2495−2502.

(107) Ramnarayanan, R.; Chan, B. C.; Salvitti, M. A.; Mallouk, T. E.; Falih, F. M.; Davis, J.; Galloway, D. B.; Bare, S. R.; Willis, R. R. *J. Comb. Chem.* **2006**, *8*, 199−212.

(108) Mallouk, T. E.; Smotkin, E. S. In *Handbook of Fuel Cells - Fundamentals, Technology and Applications*; Vielstich, W., Lamm, A., Gasteiger, H., Eds.; John Wiley & Sons, Ltd: Chichester, U.K., 2003; Vol. 2, pp 334−347.

(109) Morris, N. D.; Mallouk, T. E. *J. Am. Chem. Soc.* **2002**, *124*, 11114−11121.

(110) Chen, G. Y.; Delafuente, D. A.; Sarangapani, S.; Mallouk, T. E. *Catal. Today* **2001**, *67*, 341−355.

(111) Sun, Y. P.; Buck, H.; Mallouk, T. E. *Anal. Chem.* **2001**, *73*, 1599−1604.

(112) Reddington, E.; Sapienza, A.; Gurau, B.; Viswanathan, R.; Sarangapani, S.; Smotkin, E. S.; Mallouk, T. E. *Science* **1998**, *280*, 1735−1737.

(113) Schubert, U.; Amberg-Schwab, S.; Breitscheidel, B. *Chem. Mater.* **1989**, *1*, 2.

(114) Castillo, S.; MoranPineda, M.; Gomez, R.; Lopez, T. *J. Catal.* **1997**, *172*, 263−266.

(115) Klein, J.; Lettmann, C.; Maier, W. F. *J. Non-Cryst. Solids* **2001**, *282*, 203−220.

(116) Frenzer, G.; Maier, W. F. *Ann. Rev. Mater. Res.* **2006**, *36*, 281−331.

(117) Lin, S. D.; Vannice, M. A. *J. Catal.* **1993**, *143*, 563−572.

(118) Campanati, M.; Vaccari, A.; Piccolo, O. *J. Mol. Catal. A: Chem.* **2002**, *179*, 287−292.

(119) Sexton, B. A.; Hughes, A. E.; Foger, K. *J. Catal.* **1982**, *77*, 85−93.

(120) Longo, A.; Liotta, L. F.; Di Carlo, G.; Giannici, F.; Venezia, A. M.; Martorana, A. *Chem. Mater.* **2010**, *22*, 3952−3960.

(121) Iida, H.; Igarashi, A. *Appl. Catal., A* **2006**, *298*, 152−160.

(122) Okamoto, H. *Pt-Rh (Platinum - Rhodium) Alloy Phase Diagrams*; ASM International: Materials Park, OH, 1992; Vol. 3.